Accepted Manuscript

Title: Detection and profiling of circular RNAs in uninfected and maize Iranian mosaic virus-infected maize

Authors: Abozar Ghorbani, Keramatollah Izadpanah, Jonathan R. Peters, Ralf G. Dietzgen, Neena Mitter

PII: S0168-9452(18)30258-9
DOI: https://doi.org/10.1016/j.plantsci.2018.06.016
Reference: PSL 9885

To appear in: *Plant Science*

Received date: 1-3-2018
Revised date: 14-6-2018
Accepted date: 18-6-2018

Please cite this article as: Ghorbani A, Izadpanah K, Peters JR, Dietzgen RG, Mitter N, Detection and profiling of circular RNAs in uninfected and maize Iranian mosaic virus-infected maize, *Plant Science* (2018), https://doi.org/10.1016/j.plantsci.2018.06.016

Detection and profiling of circular RNAs in uninfected and maize Iranian mosaic virus-infected maize

Abozar Ghorbani[a,b*], Keramatollah Izadpanah[a], Jonathan R. Peters[b], Ralf G. Dietzgen[b] and Neena Mitter[b]

[a] Plant Virology Research Center, College of Agriculture, Shiraz University, Shiraz, Iran

[b] Queensland Alliance for Agriculture and Food Innovation, The University of Queensland, St. Lucia 4072, QLD, Australia

[*]**Corresponding author**: Abozar Ghorbani

E-mail address: abozar.ghorbani@shirazu.ac.ir

Telephone number: +987132286154

Highlights

- Characterization of circRNAs in maize.
- Identification and profiling of circRNAs in maize in response to MIMV infection.
- Prediction of miRNA targets of circRNAs and regulation of the transcription of parental genes by circRNAs.

Abstract

Circular RNAs (circRNAs) are covalently closed non-coding RNAs that are usually derived from exonic regions of genes, but can also arise from intronic and intergenic regions. Studies of circRNAs in humans, animals and several plant species have shown an altered population of circRNAs in response to abiotic and biotic stress. Recently it was shown that circRNAs also occur in maize, but it is unknown if maize circRNAs are responsive to stress. Maize

Iranian mosaic virus (MIMV, genus *Nucleorhabdovirus*, family *Rhabdoviridae*) causes an economically important disease in maize and other gramineous crops in Iran. In this study, we used data from RNA-Seq of MIMV-infected maize and uninfected controls to identify differentially expressed circRNAs. Such circRNAs were confirmed by two-dimensional polyacrylamide gel electrophoresis, northern blot, RT-qPCR and sequencing. A total of 1443 circRNAs were identified in MIMV-infected maize and 1165 circRNAs in uninfected maize. Two hundred and one circRNAs were in common between MIMV-infected and uninfected samples. Of these, 155 circRNAs were up-regulated and 5 down-regulated in MIMV infected plants, compared to the uninfected control. This study for the first time identified and profiled circRNA expression in maize in response to virus infection. Moreover, we predict that 33 circRNAs may bind 23 maize miRNAs, possibly affecting plant metabolism and development. Our data suggest a role for circRNAs in plant cell regulation and response to biotic stress such as virus infection, and give new insights into the complexity of plant-microbe interactions.

Key words: Circular RNAs, plant gene regulation, Maize, MIMV, RNA-Seq

1. Introduction

Endogenous circular RNAs (circRNAs) were first identified from the human *Ets* gene, processed from pre-mRNAs [1]. CircRNAs are formed by covalent linkage between an upstream splice acceptor and a downstream splice donor of the same RNA molecule in a process known as back-end splicing [2]. The formation of circRNAs is considered a rare event [2-5]. ALU repeat elements (AGCT) are often associated with circRNAs, flanking the splice junction.

Recently, rRNA depleted RNA-Seq (Ribominus-Seq) was used to study circRNAs in human and plant cells [6-10]. These studies showed specific expression patterns of circRNAs in different tissues, cell-types and developmental stages [2, 9, 11]. Studies of circRNAs by aligning RNA-Seq reads to model plant transcriptomes revealed 12,037 circRNAs in rice (*Oryza sativa)* and 6012 in *Arabidopsis thaliana* [6, 7]. Plant circRNAs are generated from various genomic regions, but mainly from coding regions [12]. CircRNAs exist in both monocot and dicot plant species and have been studied in Arabidopsis, wheat, barley, tomato, soybean and rice [6, 12, 13].

Although there is some disagreement on the function of circRNAs, some studies suggest that they have an important role in transcriptional and post-transcriptional regulation by interacting with miRNAs [14-18]. CircRNAs in rice may function as negative regulators by reducing the expression level of their parental genes [19]. They may also act as positive regulators of their parental genes by interacting with and "sponging" miRNAs. Previous studies on exonic and intronic splicing have revealed novel isoforms with aberrant expression under conditions of environmental stress [20], suggesting a potential role for circRNAs in stress response [7]. At this time, there is no information on the potential effect of virus infection on circRNA populations in plants.

Maize Iranian mosaic virus (MIMV) is a nucleorhabdovirus that infects maize plants in Iran [21, 22]. It is transmitted by the small brown planthopper (*Laodelphax striatellus* L.) in a persistent-propagative manner [23, 24]. In this study, circRNAs including those with differential expression were identified for the first time in healthy maize and in MIMV-infected plants. To identify maize circRNAs, we analyzed RNA-Seq data from MIMV-infected and uninfected maize total RNA.

2. Materials and Methods

2.1. Plant growth, virus inoculation and RNA extraction.

Seeds of MIMV-susceptible maize cultivar 704 (Agriculture and Natural Resources Research Center of Fars, Shiraz, Iran) were germinated in soil, and plants were grown in a greenhouse on a cycle of 16 h light at 30˚C and 8 h dark at 25˚C. Three days after seed germination, at the two-leaf stage, ten maize plants were exposed for 3 days to 20 viruliferous planthopper nymphs that had been maintained on MIMV-infected barley plants in an insect-proof cage and were infected with Fars isolate of MIMV. Mock-inoculated plants were exposed to 20 planthoppers from a virus-free colony on barley. Total RNA was extracted from 500 mg of leaf tissue using TRIzol Reagent (Thermo Fisher Scientific) following the manufacturer's instructions. Samples for RNA extraction included three uninfected and three infected plants, 15 days after inoculation when symptoms were visible. The total RNA was dissolved in diethyl pyrocarbonate-treated water, and the purity of RNA extracts was assessed by measuring absorption ratio A260/280 with a Nanodrop-1000 spectrophotometer (Thermo Scientific, Wilmington, DE, USA). Quality and integrity of the RNA was assessed by 1% (w/v) agarose gel electrophoresis in Tris/borate/EDTA (TBE) buffer.

2.2. Virus detection.

MIMV was detected in maize plants by Double Antibody Sandwich (DAS)-ELISA using MIMV-specific antiserum [25] as described by Converse and Martin (1990) [26]. Alternatively, MIMV was detected using RT-PCR with primers MIMV-F 5′-TGCAGGGAAATCTCTGGAGG-3′ and MIMV-R 5′-CCTCATACATTGGCTGGGGA-3′. Complementary DNA was synthesized using M-MLV reverse transcriptase (Thermo Fisher Scientific) and primer MIMV-R. PCR was done in a total reaction volume of 25 µL (Cinnagen, Iran) following the manufacturer's instructions in a BioRad thermal cycler.

2.3. Library construction, sequencing and RNA-Seq data analysis.

Following quality control with Bioanalyzer (Agilent Technologies 2100) using a DNA 1000 chip and Roche's Rapid library standard Quantification solution and calculator, passed samples were used in library construction (TruSeq RNA Sample Prep Kit v2) and sequenced with 100 bp paired end reads using Illumina HiSeq 2500 (Macrogen, Seoul, South Korea). Contaminating genomic DNA was removed during mRNA purification. Whole transcriptome RNA was enriched by Macrogen by depleting ribosomal RNA, and six independent cDNA libraries were prepared using poly(A) enrichment from 3 plants each of MIMV-infected and non-infected maize [27].

2.4. Bioinformatics analysis.

To systematically identify maize circRNAs, a rigorous bioinformatics pipeline was set up following design principles described in previous studies [2, 8]. Ribominus-Seq reads were first mapped to maize reference genomes (www.plants.ensembl.org) using BOWTIE2 (v2.0.5) [28] with the same parameters used by Memczak et al. (2013) and matching reads were discarded. From the remaining unmapped reads, we extracted 20-nt anchors from both ends and aligned them independently to the reference genomes to find unique anchor positions. Presence of aligned anchors in reverse orientation indicated circRNA splicing. The anchor alignments were then extended such that the complete read could be aligned and that the breakpoints were flanked by GU/AG splice sites. A candidate circRNA

was called if it was supported by at least two unique back-spliced reads [6]. Transcriptome reads were mapped to candidate circRNAs by CLC Genomic Workbench version 9 (CLC Bio, Qiagen). Quantification of gene expression was done using the RPKM (Reads per kilobase of transcript per million mapped reads) algorithm. MATLAB software (R2014a) was used to identify circRNAs that were common between MIMV-infected maize and uninfected maize. Size distribution of circRNAs was determined by Microsoft Excel software 2013. CLC Genomic Workbench version 10 was used to predict circRNAs secondary structure. A heat map was generated for the number of circRNAs in each chromosome and differential expression of circRNAs by Heatmapper online software (http://www2.heatmapper.ca/expression/). CircRNAs were blasted against the maize microRNA database (http://www.mirbase.org/) using CLC Genomic Workbench to identify cognate miRNAs. The gene origins of circRNAs were determined by Ensembl Plants database (www. http://plants.ensembl.org) and Gene Ontology analysis was done using BLAST2GO version 4. We intend to deposit the circRNA data in a suitable database with the name of maize circRNAs in response to MIMV.

2.5. Two-dimensional gel electrophoresis and RNA blotting.

RNA was mixed 1:1 (v/v) with loading dye (95% formamide, 18 mM EDTA, 0.025% SDS, xylene cyanol and bromophenol blue), incubated at 95°Ċ for 4 min, cooled on ice and separated on a 3% polyacrylamide gel containing 8M urea/TBE until the bromophenol blue dye front reached the end of the gel. The entire lane in which RNA had been separated was cut from the gel and placed in a perpendicular orientation at the head of a second 6% polyacrylamide gel in TBE, and RNA was separated in the second dimension then stained with ethidium bromide and detected by UV light. CircRNA primers (Table 1) were labeled with digoxigenin using DIG oligonucleotide 3´-end labeling kit (Roche, Merck) following the manufacturer's instructions. RNA was transferred to Nytran Super Charge nylon membrane (Schleicher & Schüll BioScience) by Trans-Blot® SD Semi-Dry Transfer Cell (Bio-Rad) and cross-linked by UV irradiation at 1200 mJ in a Stratagene UV Crosslinker. Hybridization and washing was done following the manufacturer's protocol for DIG hybridization. CircRNAs were detected by non-radioactive chemi-luminescent northern detection protocol (adapted from "DIG Filter Hyb Manual", Roche).

2.6. Validation of circRNAs by quantitative PCR.

Five circRNAs that showed differential expression (DE) between MIMV-infected maize and control were selected for validation by RT-qPCR. Ubiquitin-conjugating enzyme and cullin were selected as internal reference genes from the non-DE genes in the RNA-Seq dataset. Convergent and divergent PCR primers (Table 1) were designed using Primer 3 software in Geneious version R10 (Biomatters, New Zealand) and synthesized by GeneWorks (Adelaide, South Australia). Independent total RNA extracts from MIMV-infected and uninfected maize plants, 15 days after MIMV inoculation were used, as for RNA extractions for RNA-Seq. Total RNA was treated with DNase (Ambion, TURBO DNA-free). Linear RNAs were digested using RNase R (20 U/µl) (Epicentre, Illumina, San Diego, CA, USA) for 15 minutes at 37°Ċ following the manufacturer's protocol. First-strand cDNA was synthesized using random hexamer primers and Superscript III First-strand cDNA synthesis kit (Life Technologies). SensiFAST SYBR No-ROX Kit (Bioline) was used in a Rotor-Gene Q real-time PCR cycler (Qiagen) following manufacturer's protocol with 20 µl reactions containing 20 ng cDNA and 10 µM of each primer. QPCR cycling conditions were: 95°C for 2 min, 40 cycles of 94°C for 5 sec, 55°C for 10 sec and 72°C for 20 sec. Three biological replicates and two technical replicates were used for each sample. Threshold cycle (Ct) number was calculated from log scale amplification curves by Rotor-Gene Q Series software. Differential expression for these circRNAs in qPCR was calculated using divergent primers. Since circRNAs do not have a poly (A) tail, random primers were used for first strand cDNA synthesis. To distinguish circular RNA from their linear counterparts in qPCR, the forward and reverse primers were situated in the two separate exons that are joined together at the circular junction site to form circular RNA, such that the amplicon spans the circular junction. The directions of the primers face toward each other for the circRNA sequence but away from each other for the linear RNA, also referred to as "outward facing" or "divergent" primers. The linear housekeeping genes, ubiquitin-conjugating enzyme and cullin in samples without RNase R treatment were used as qPCR normalization references. The differential expression of circular RNA was calculated by the "ΔΔCt" method [29]. Real-time PCR products were directly sequenced for confirmation using divergent and convergent primers.

3. Result and Discussion

3.1. Virus detection.

Plants grown under greenhouse conditions displayed typical MIMV symptoms 15 days after planthopper-mediated infection. MIMV-infected seedlings were stunted and leaves showed yellow stripes. The presence of MIMV in inoculated plants and it absence in mock-inoculated plants was confirmed by DAS-ELISA and RT-PCR (data not shown).

3.2. Identification and profiling of circRNAs in maize in response to MIMV infection.

The initial discovery and characterization of circRNAs has relied on biochemical methods such as reverse transcription-PCR [30]. In recent years, advances in sequencing technology combined with powerful bioinformatics and statistical approaches have been used to identify and quantify the expression of a much greater number of circRNAs with high confidence [30]. In this study, we identified circRNAs in maize RNA-Seq data generated from rRNA-depleted samples. rRNA-depleted or total RNA libraries have been most commonly used [6, 19, 31] for circRNA profiling. Six cDNA libraries were constructed for deep sequencing using the Illumina High-Seq 2500 platform. After removal of adaptor sequences about 42 million clean reads were obtained for each sample. The Illumina sequence read data are accessible through the NCBI BioProject database with accessions numbers SAMN08237478 – SAMN08237483. CircRNAs were identified based on back-spliced reads in rRNA-depleted RNA-Seq (Ribominus-Seq) data of MIMV-infected maize and uninfected maize. In a recent study, Chen and collaborators uncovered 2804 circRNAs in maize leaves generated from transposons and associated with phenotypic variation [32]. In the present study, 1443 circRNAs unique to MIMV-infected maize and 1165 circRNAs unique to uninfected maize were identified (Fig. 1). Two hundred and one circRNAs were in common to MIMV-infected and uninfected maize (Fig. 1). In previous studies, 12,037 and 2354 circRNAs were identified from rice, 6012 from *Arabidopsis thaliana*, 854 from tomato, 62 from barley and 88 from wheat by analyzing publically available RNA-Seq data [6, 12, 19, 33, 34].

3.3. Characterization of circRNAs in maize.

CircRNAs were derived from all 10 chromosomes of the maize genome. Chromosome 10 showed the highest number of circRNA loci that are expressed in both MIMV-infected and uninfected maize. Chromosome 1 contained

the most circRNA loci in both MIMV-infected and uninfected maize, whereas we identified more circRNAs on chromosomes 4 and 5 from MIMV-infected maize compared to uninfected maize (Fig. 2). Hierarchical cluster analysis showed that chromosomes 3 and 6 had circRNA loci patterns similar to chromosome 7. These results show a shift in the chromosomal location of the predominantly expressed circRNA loci in response to MIMV infection. Similarly in mammalian cells, three chromosomes in human testes had more circRNA loci than the other chromosomes [35]. Furthermore, different distribution patterns of circRNAs in the rat genome were reported during liver regeneration [36]. CircRNAs were found to be widely and unevenly transcribed across pig chromosomes [37]. This type of analysis has not been reported for any plant species. Taken together, our results indicate that active circRNA loci are distributed across all maize chromosomes and that their distribution appears to be influenced by ~~to~~ cellular stress conditions. Maize circRNAs in this study and the recent transposon study [32] showed common features similar to circRNAs identified in other plant species.

About 85% of circRNAs identified in MIMV-infected and uninfected maize were 120-300 nt, although some circRNAs were more than 10,000 nt (Fig. 3). Similarly, the most frequent size class of circRNAs in human testis and pig were 200-400 nt, with a small number of circRNAs larger than 5000 nt [35, 37]. Secondary structures have important roles in the functions of non-coding RNAs, for example stem loops can interact with some proteins [38]. We therefore analyzed circRNA secondary structure *in silico* using prediction algorithms to identify presence of hairpin loops, interior loops, stems, bulges and multi-loops. Such structures may have a potential role in circRNA function, because for example stem-loops are recognized by RNA binding proteins [39]. The combination of being covalently closed at both ends and secondary structure makes circRNAs more stable and less prone to degradation compared to linear RNA [8]. This increased stability may allow circRNAs to remain functional longer in response to biotic or abiotic stresses [40].

CircRNAs have structural similarities with viroids, virus-like noncoding circular RNAs with a high degree of secondary structure that cause diseases in plants by interacting with miRNAs and host proteins [39, 41, 42]. Viroids can move independently cell-to-cell and also traffic long-distance based on various RNA motifs. Viroid sequence motifs control phloem trafficking and have been shown to interact with some host proteins to facilitate cell-to-cell movement [39, 41, 42]. Based on the similarities with viroids, it is tempting to speculate that circRNAs may also traffic short and long distances between plant cells.

The majority of plant circRNAs reported thus far exhibit differential expression patterns in several plant species in response to abiotic and biotic stress and at different stages of plant development [34, 39, 43]. We analyzed circRNAs common to uninfected and infected samples (Fig. 1B) and found that they were differentially expressed in response to infection. In total, 155 maize circRNAs were up-regulated (fold change > 2, p-value <0.05) and five circRNAs were down-regulated (fold change < -2, p-value <0.05) in response to MIMV infection (Fig. 4).

Other studies have shown circRNAs to be differentially expressed (DE) in response to environmental stress. For instance, 27 rice circRNAs were DE under phosphate-sufficient and -starvation conditions [6]. Eighty-eight circRNAs were identified in leaves of wheat seedlings and 62 of them were DE in water-stressed seedlings compared to well-watered controls [12], and 163 circRNAs were up-regulated in response to chilling in tomato [34].

3.4. Prediction of miRNA targets of circRNAs and regulation of the transcription of parental genes by circRNAs.

CircRNAs can regulate miRNA accumulation through binding and sequestration [44]. Binding between circRNA and miRNA is based on sequence complementarity. Hence, to predict circRNAs with potential miRNA regulatory function, we searched the circRNAs and their complementary sequences against the maize miRNA database using BLAST algorithm, and found that 33 circRNAs were complementary to 23 miRNAs (Table 2). The function of the majority of these miRNAs is unknown. However, we found one circRNA 2:1923979-1970968 that was complementary to miR399, identified in *A. thaliana*, maize and rice, and that is known to play a role in regulation of mRNAs coding for a phosphate transporter [45, 46]. Furthermore, circRNA 2:55894943-55895081 sequence was 100% complementary to miR172 that regulates mRNAs coding for APETALA2-like transcription factors, involved in floral development [45, 47]. Other reports suggest that some circRNAs may be target mimics for miR172 and miR810 [19]. Another circRNA found on chromosome 5 (5:161330154-161330300) is 95.5% complementary to miR160, which has been identified in a range of plant species, including *A. thaliana*, maize and rice. miR160 is known to bind to sites in the untranslated regions of auxin response factor genes [45, 47]. miRNAs families MIR396, MIR2118, MIR166 and MIR159 are listed in Table 2 [45, 46, 48]. Taken together, our investigation has identified sequence complementarity between MIMV-responsive circRNAs and a number of maize miRNAs, involved in regulating developmental genes, suggesting that MIMV activation of circRNAs may affect a number of cellular processes through miRNA sequestration.

Previous studies have shown that circRNAs regulate the transcription of parental genes in the nucleus [49]. Additionally, it was shown in rice that transgenic expression of circRNAs could act as negative post-transcriptional regulators, and reduce the expression level of parental genes [19]. We determined the parental genes of maize circRNAs from their location in chromosomes where they were derived. Gene ontology of cellular components of parental genes in MIMV-infected maize showed that most of the gene products are predicted to reside in the nucleus, chloroplast and as integral components in membrane (Supplementary Fig 1). Presence of most MIMV proteins in the nucleus and plasma membrane [49] suggests the role of circRNAs in response to MIMV infection. Also, MIMV shows symptoms such as mosaic and chlorotic veins which may be related to parental genes of circRNAs in chloroplasts. Biological process analysis highlighted genes that were involved in regulation of glutamate metabolic process and response to stimulus. Such biological regulations were observed in MIMV infected and uninfected samples (Supplementary Fig 2). Oxidoreductase and ubiquitin-protein transferase activity genes featured in the molecular function analysis in the MIMV-infected samples (Supplementary Fig 3). These processes are known to be related to stress responses in plants [50, 51] suggesting a regulatory role of circRNAs in maize in response to MIMV infection.

3.5. Validation of circRNAs by 2-D gel electrophoresis and northern blot

2-D denaturing polyacrylamide gel electrophoresis (PAGE) provides a means to separate and distinguish circular forms of RNAs from linear RNA in a sample of total RNA [52]. When total RNA is separated consecutively on two different concentrations of polyacrylamide in two dimensions, linear RNAs migrate as a diagonal line whereas circRNAs do not owing to their structure [30, 52]. Total RNA from MIMV-infected maize separated on 2-D PAGE was visualized by ethidium bromide staining and UV light showed a characteristic diagonal line (Fig. 5a), whereas the presence of a characteristic "arc" representing circRNAs was not detectable by ethidium bromide staining, likely due to low detection sensitivity and/or low circRNA concentration relative to linear RNAs. To increase sensitivity of circRNA detection, we transferred RNA that had been treated with RNase R (to digest linear RNAs) on 2-D PAGE to a nylon membrane for northern blotting, using a mixture of all circRNA primers (Table 1) in equal amounts as probes targeting the circularized exonic sequence spanning the splice junction [30]. Northern blot showed an "arc", confirming presence of circRNAs in total RNA extracted from MIMV-infected maize (Fig. 5b).

3.6. Validation of circRNAs by quantitative PCR

Quantitative RT-PCR of RNase R-treated RNA extracts using divergent primers confirmed the bioinformatics analysis of the RNA-Seq data and yielded a measure of relative circRNA abundance. RNase R is a 3' to 5' exoribonuclease specific for single stranded linear RNAs or some double stranded linear RNAs with free 3' single stranded overhangs and cannot degrade covalently closed circRNAs, thereby RNase R treatment of total RNA enables enrichment for circRNAs [53, 54]. Randomly primed cDNA derived from circRNA contains diagnostic exon-exon junction sequences that are absent in canonically spliced mRNAs, and divergent primers can amplify across these junctions [30]. The convergent primers on the other hand amplify the linear and circular forms of the exon, and forward and reverse primers face towards each other on the linear exon sequence. QPCR analysis using divergent and convergent primers validated up-regulation of five circRNA candidates identified from our sequencing data, although Pearson correlation was low probably because extracts from different plants were used for RNA-Seq and qPCR (Fig. 7). Direct sequencing of the amplicons demonstrated the specificity of RT-qPCR results (data not shown). These results support our finding that circRNAs are expressed/transcribed in response to MIMV infection in maize.

4.0 Conclusions

CircRNAs are generated in maize and some are responsive to infection by the nucleorhabdovirus maize Iranian mosaic virus. The functions of these circRNAs are not well understood but they likely regulate miRNAs and parental genes in maize that are involved in stress responses.

Author contributions

AG, KI, RD and NM designed the study; AG and JP performed the experiments, AG analysed the data and drafted the manuscript, all authors edited and approved the final version of the manuscripts.

Formatting of funding sources

This research was jointly supported by the Queensland Department of Agriculture and Fisheries and the University of Queensland through the Queensland Alliance for Agriculture and Food Innovation. Funds for RNA-Seq and preliminary experiments were provided by Plant Virology Research Center, College of Agriculture, Shiraz University.

Acknowledgements

AG was supported by a scholarship from Shiraz University, Iran and Iranian Council of Centers of Excellence and National Foundation of Elites. The authors wish to thank Saied Babai and Stephen Fletcher for technical advice.

References

[1] J.M. Nigro, K.R. Cho, E.R. Fearon, S.E. Kern, J.M. Ruppert, J.D. Oliner, K.W. Kinzler, B. Vogelstein, Scrambled exons, Cell, 64 (1991) 607-613.
[2] S. Memczak, M. Jens, A. Elefsinioti, F. Torti, J. Krueger, A. Rybak, L. Maier, S.D. Mackowiak, L.H. Gregersen, M. Munschauer, Circular RNAs are a large class of animal RNAs with regulatory potency, Nature, 495 (2013) 333-338.
[3] W.R. Jeck, J.A. Sorrentino, K. Wang, M.K. Slevin, C.E. Burd, J. Liu, W.F. Marzluff, N.E. Sharpless, Circular RNAs are abundant, conserved, and associated with ALU repeats, RNA, 19 (2013) 141-157.
[4] S. Starke, I. Jost, O. Rossbach, T. Schneider, S. Schreiner, L.-H. Hung, A. Bindereif, Exon circularization requires canonical splice signals, Cell Reports, 10 (2015) 103-111.
[5] S.P. Barrett, P.L. Wang, J. Salzman, Circular RNA biogenesis can proceed through an exon-containing lariat precursor, Elife, 4 (2015) e07540.
[6] C.Y. Ye, L. Chen, C. Liu, Q.H. Zhu, L. Fan, Widespread noncoding circular RNAs in plants, New Phytologist, 208 (2015) 88-95.
[7] G. Sablok, H. Zhao, X. Sun, Plant circular RNAs (circRNAs): transcriptional regulation beyond miRNAs in plants, Molecular plant, 9 (2016) 192-194.
[8] W.R. Jeck, N.E. Sharpless, Detecting and characterizing circular RNAs, Nature Biotechnology, 32 (2014) 453-461.
[9] J. Salzman, R.E. Chen, M.N. Olsen, P.L. Wang, P.O. Brown, Cell-type specific features of circular RNA expression, Plos Genetics, 9 (2013) e1003777.
[10] J. Salzman, C. Gawad, P.L. Wang, N. Lacayo, P.O. Brown, Circular RNAs are the predominant transcript isoform from hundreds of human genes in diverse cell types, PloS one, 7 (2012) e30733.
[11] Y. Gao, J. Wang, F. Zhao, CIRI: an efficient and unbiased algorithm for de novo circular RNA identification, Genome Biology, 16 (2015) 4.
[12] Y. Wang, M. Yang, S. Wei, F. Qin, H. Zhao, B. Suo, Identification of circular RNAs and their targets in leaves of Triticum aestivum L. under dehydration stress, Frontiers in Plant Science, 7 (2016).
[13] W. Zhao, Y. Cheng, C. Zhang, Q. You, X. Shen, W. Guo, Y. Jiao, Genome-wide identification and characterization of circular RNAs by high throughput sequencing in soybean, Scientific Reports, 7 (2017) 5636.
[14] J.M. Franco-Zorrilla, A. Valli, M. Todesco, I. Mateos, M.I. Puga, I. Rubio-Somoza, A. Leyva, D. Weigel, J.A. García, J. Paz-Ares, Target mimicry provides a new mechanism for regulation of microRNA activity, Nature Genetics, 39 (2007) 1033-1037.
[15] M.S. Ebert, J.R. Neilson, P.A. Sharp, MicroRNA sponges: competitive inhibitors of small RNAs in mammalian cells, Nature Methods, 4 (2007) 721-726.
[16] F. Gualandi, C. Trabanelli, P. Rimessi, E. Calzolari, L. Toffolatti, T. Patarnello, G. Kunz, F. Muntoni, A. Ferlini, Multiple exon skipping and RNA circularisation contribute to the severe phenotypic expression of exon 5 dystrophin deletion, Journal of Medical Genetics, 40 (2003) e100-e100.
[17] C.W. Chao, D.C. Chan, A. Kuo, P. Leder, The mouse formin (Fmn) gene: abundant circular RNA transcripts and gene-targeted deletion analysis, Molecular Medicine, 4 (1998) 614.
[18] C.-y. Chen, P. Sarnow, Initiation of protein synthesis by the eukaryotic translational apparatus on circular RNAs, Science, 268 (1995) 415.
[19] T. Lu, L. Cui, Y. Zhou, C. Zhu, D. Fan, H. Gong, Q. Zhao, C. Zhou, Y. Zhao, D. Lu, Transcriptome-wide investigation of circular RNAs in rice, RNA, 21 (2015) 2076-2087.
[20] X.J. Min, B. Powell, J. Braessler, J. Meinken, F. Yu, G. Sablok, Genome-wide cataloging and analysis of alternatively spliced genes in cereal crops, BMC Genomics, 16 (2015) 721.
[21] A.O. Jackson, R.G. Dietzgen, M.M. Goodin, J.N. Bragg, M. Deng, Biology of plant rhabdoviruses, Annual Review of Phytopathology., 43 (2005) 623-660.
[22] K. Izadpanah, A. Ahmadi, S. Parvin, S. Jafari, Transmission, particle size and additional hosts of the rhabdovirus causing maize mosaic in Shiraz, Iran, Journal of Phytopathology, 107 (1983) 283-288.
[23] A. Massah, K. Izadpanah, A. Afsharifar, S. Winter, Analysis of nucleotide sequence of Iranian maize mosaic virus confirms its identity as a distinct nucleorhabdovirus, Archives of Virology, 153 (2008) 1041-1047.
[24] A. Massah, K. Izadpanah, D. Lesemann, Relationship of Iranian maize mosaic virus with insect vector and plant cells, Iranian Journal of Plant Pathology, 41 (2005) 151-159.

[25] K. Izadpanah, Purification and serology of the Iranian maize mosaic rhabdovirus, Journal of Phytopathology, 126 (1989) 43-50.
[26] R. Converse, R. Martin, Enzyme-linked immunosorbent assay (ELISA), Serological methods for detection and identification of viral and bacterial plant pathogens, (1990) 179-196.
[27] A. Ghorbani, K. Izadpanah, R.G. Dietzgen, Changes in maize transcriptome in response to maize Iranian mosaic virus infection, Plos one, 13 (2018) e0194592.
[28] B. Langmead, S.L. Salzberg, Fast gapped-read alignment with Bowtie 2, Nature Methods, 9 (2012) 357.
[29] K.J. Livak, T.D. Schmittgen, Analysis of relative gene expression data using real-time quantitative PCR and the 2− ΔΔCT method, Methods, 25 (2001) 402-408.
[30] S.P. Barrett, J. Salzman, Circular RNAs: analysis, expression and potential functions, Development, 143 (2016) 1838-1847.
[31] H.-Z. Li, X. Gao, X.-Y. Li, Q.-J. Chen, J. Dong, W.-C. Zhao, Evaluation of assembly strategies using RNA-seq data associated with grain development of wheat (Triticum aestivum L.), Plos One, 8 (2013) e83530.
[32] L. Chen, P. Zhang, Y. Fan, Q. Lu, Q. Li, J. Yan, G.J. Muehlbauer, P.S. Schnable, M. Dai, L. Li, Circular RNAs mediated by transposons are associated with transcriptomic and phenotypic variation in maize, New Phytologist, 217 (2018) 1292-1306.
[33] Y. Wang, Q. Wang, L. Gao, B. Zhu, Y. Luo, Z. Deng, J. Zuo, Integrative analysis of circRNAs acting as ceRNAs involved in ethylene pathway in tomato, Physiologia Plantarum, (2017).
[34] J. Zuo, Q. Wang, B. Zhu, Y. Luo, L. Gao, Deciphering the roles of circRNAs on chilling injury in tomato, Biochemical and Biophysical Research Communications, 479 (2016) 132-138.
[35] W.-W. Dong, H.-M. Li, X.-R. Qing, D.-H. Huang, H.-G. Li, Identification and characterization of human testis derived circular RNAs and their existence in seminal plasma, Scientific Reports, 6 (2016) 39080.
[36] L. Li, J. Guo, Y. Chen, C. Chang, C. Xu, Comprehensive CircRNA expression profile and selection of key CircRNAs during priming phase of rat liver regeneration, BMC Genomics, 18 (2017) 80.
[37] G. Liang, Y. Yang, G. Niu, Z. Tang, K. Li, Genome-wide profiling of Sus scrofa circular RNAs across nine organs and three developmental stages, DNA Research, (2017).
[38] C.P. Ponting, P.L. Oliver, W. Reik, Evolution and functions of long noncoding RNAs, Cell, 136 (2009) 629-641.
[39] Q.-F. Li, Y.-C. Zhang, Y.-Q. Chen, Y. Yu, Circular RNAs roll into the regulatory network of plants, Biochemical and Biophysical Research Communications, 488 (2017) 382-386.
[40] Y. Li, Q. Zheng, C. Bao, S. Li, W. Guo, J. Zhao, D. Chen, J. Gu, X. He, S. Huang, Circular RNA is enriched and stable in exosomes: a promising biomarker for cancer diagnosis, Cell Research, 25 (2015) 981.
[41] B. Ding, A. Itaya, X. Zhong, Viroid trafficking: a small RNA makes a big move, Current Opinion in Plant Biology, 8 (2005) 606-612.
[42] Y. Wang, B. Ding, Viroids: small probes for exploring the vast universe of RNA trafficking in plants, Journal of Integrative Plant Biology, 52 (2010) 28-39.
[43] H.-J. Wu, Z.-M. Wang, M. Wang, X.-J. Wang, Widespread long noncoding RNAs as endogenous target mimics for microRNAs in plants, Plant Physiology, 161 (2013) 1875-1884.
[44] Q. Zheng, C. Bao, W. Guo, S. Li, J. Chen, B. Chen, Y. Luo, D. Lyu, Y. Li, G. Shi, Circular RNA profiling reveals an abundant circHIPK3 that regulates cell growth by sponging multiple miRNAs, Nature Communications, 7 (2016).
[45] L. Zhang, J.-M. Chia, S. Kumari, J.C. Stein, Z. Liu, A. Narechania, C.A. Maher, K. Guill, M.D. McMullen, D. Ware, A genome-wide characterization of microRNA genes in maize, Plos Genetics, 5 (2009) e1000716.
[46] T. Dezulian, J.F. Palatnik, D. Huson, D. Weigel, Conservation and divergence of microRNA families in plants, Genome Biology, 6 (2005) P13.
[47] C. Maher, M. Timmermans, L. Stein, D. Ware, Identifyng microRNAs in plant genomes, in: Computational Systems Bioinformatics Conference, 2004. CSB 2004. Proceedings. 2004 IEEE, IEEE, 2004, pp. 718-723.
[48] C. Johnson, A. Kasprzewska, K. Tennessen, J. Fernandes, G.-L. Nan, V. Walbot, V. Sundaresan, V. Vance, L.H. Bowman, Clusters and superclusters of phased small RNAs in the developing inflorescence of rice, Genome Research, 19 (2009) 1429-1440.
[49] Z. Li, C. Huang, C. Bao, L. Chen, M. Lin, X. Wang, G. Zhong, B. Yu, W. Hu, L. Dai, Exon-intron circular RNAs regulate transcription in the nucleus, Nature Structural & Molecular Biology, 22 (2015) 256-264.
[50] A. Ghorbani, K. Izadpanah, R.G. Dietzgen, Gene expression and population polymorphism of maize Iranian mosaic virus in *Zea mays*, and intracellular localization and interactions of viral N, P, and M proteins in *Nicotiana benthamiana*, Virus Genes, 54 (2018) 290-296.

[51] K. Pageau, M. Reisdorf-Cren, J.-F. Morot-Gaudry, C. Masclaux-Daubresse, The two senescence-related markers, GS1 (cytosolic glutamine synthetase) and GDH (glutamate dehydrogenase), involved in nitrogen mobilization, are differentially regulated during pathogen attack and by stress hormones and reactive oxygen species in Nicotiana tabacum L. leaves, Journal of Experimental Botany, 57 (2005) 547-557.
[52] H. Tabak, G. Van der Horst, J. Smit, A. Winter, Y. Mul, G.M. Koerkamp, Discrimination between RNA circles, interlocked RNA circles and lariats using two-dimensional polyacrylamide gel electrophoresis, Nucleic Acids Research, 16 (1988) 6597-6605.
[53] H. Suzuki, Y. Zuo, J. Wang, M.Q. Zhang, A. Malhotra, A. Mayeda, Characterization of RNase R-digested cellular RNA source that consists of lariat and circular RNAs from pre-mRNA splicing, Nucleic Acids Research, 34 (2006) e63-e63.
[54] H.A. Vincent, M.P. Deutscher, Substrate Recognition and Catalysis by the Exoribonuclease RNase R, Journal of Biological Chemistry, 281 (2006) 29769-29775.

Figure legends

Fig 1. Unique (A, C) and shared (B) circRNAs in uninfected maize (A) and MIMV-infected maize (C).

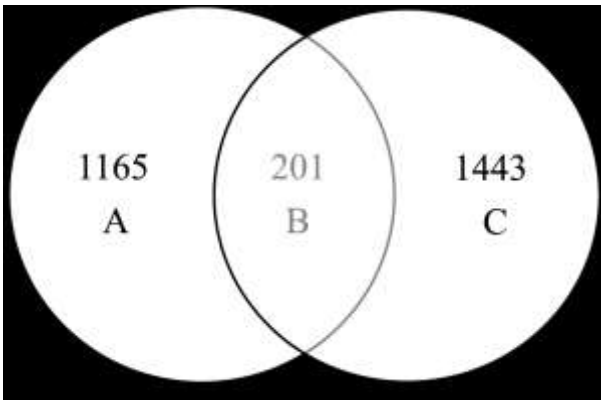

Fig 2. Heat map and hierarchical cluster analysis of circRNAs detected in MIMV-infected maize, uninfected maize and common to both of them. Abundance of circRNA loci is indicated by the heat map scale increasing from green to red and numbers on the left (number of circRNA per chromosome). Numbers on the right show the chromosome number of maize.

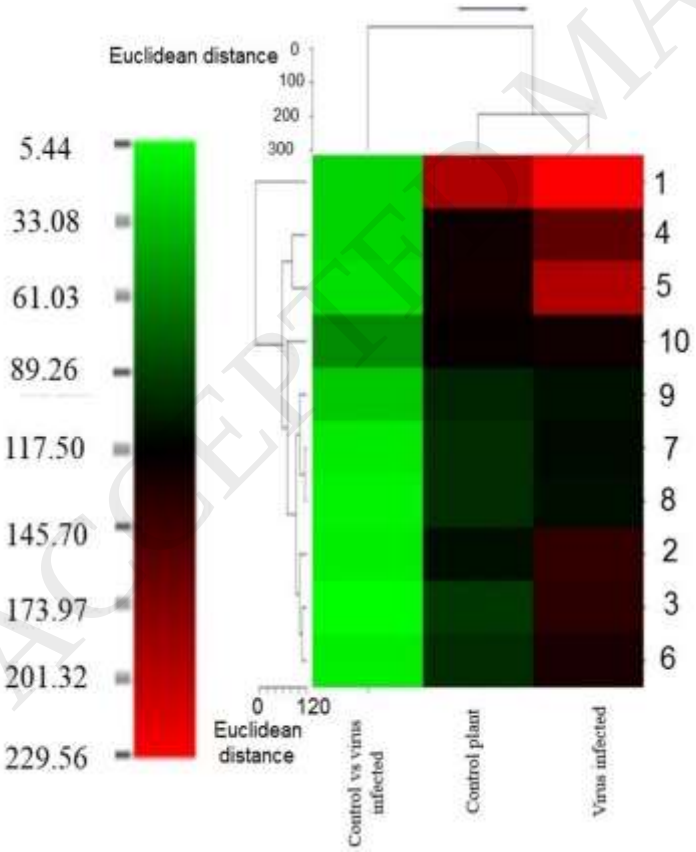

Fig 3. Size distribution of full-length circRNAs from maize. X-axis: length in nucleotides (nt); Y-axis: frequency of fragments of each length class. a. Infected maize. b. Uninfected maize.

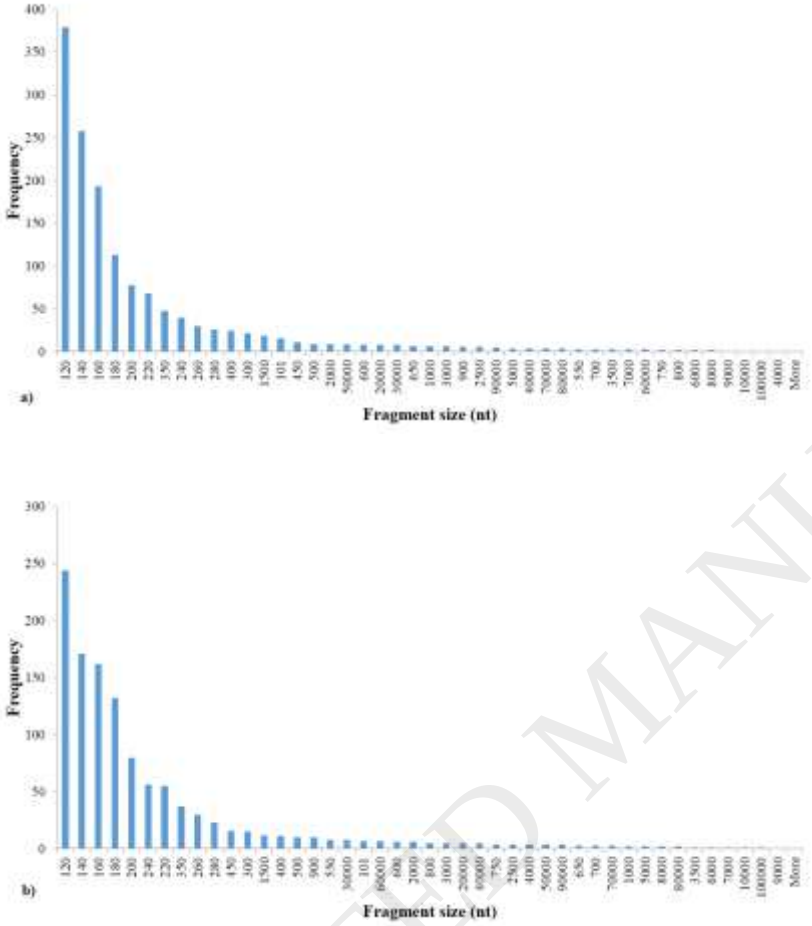

Fig 4. Heat map and hierarchical cluster analysis showing differential expression of circRNAs in MIMV-infected and uninfected maize. Heat map row Z-score shown at top left. Z-score is the number of standard deviations an observation is from the mean; at a Z-score of zero, the score and mean are equal.

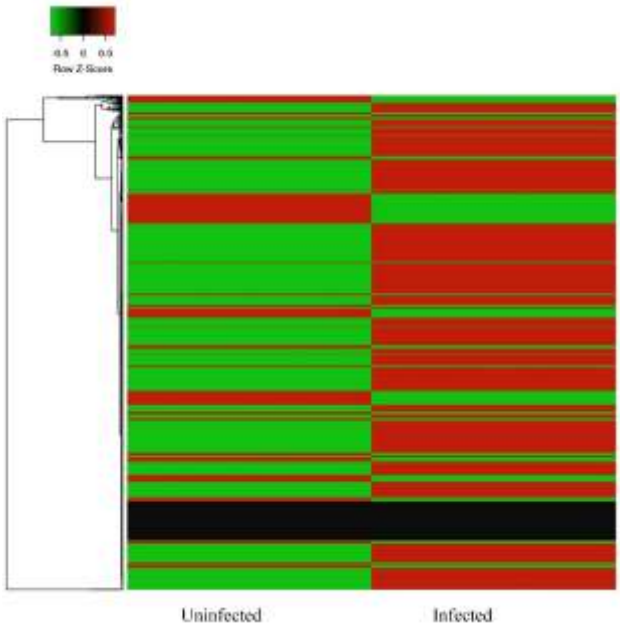

Fig 5. Detection of linear and circular RNAs in total RNA extracted from MIMV-infected maize by two-dimensional gel electrophoresis. a. Linear RNAs visualized by ethidium bromide staining. b. CircRNAs detected in RNase R treated total RNA using an equal mixture of all circRNA primers (Table 1) as probes. Arrows indicates the direction of electrophoretic separation in the first and second dimensions.

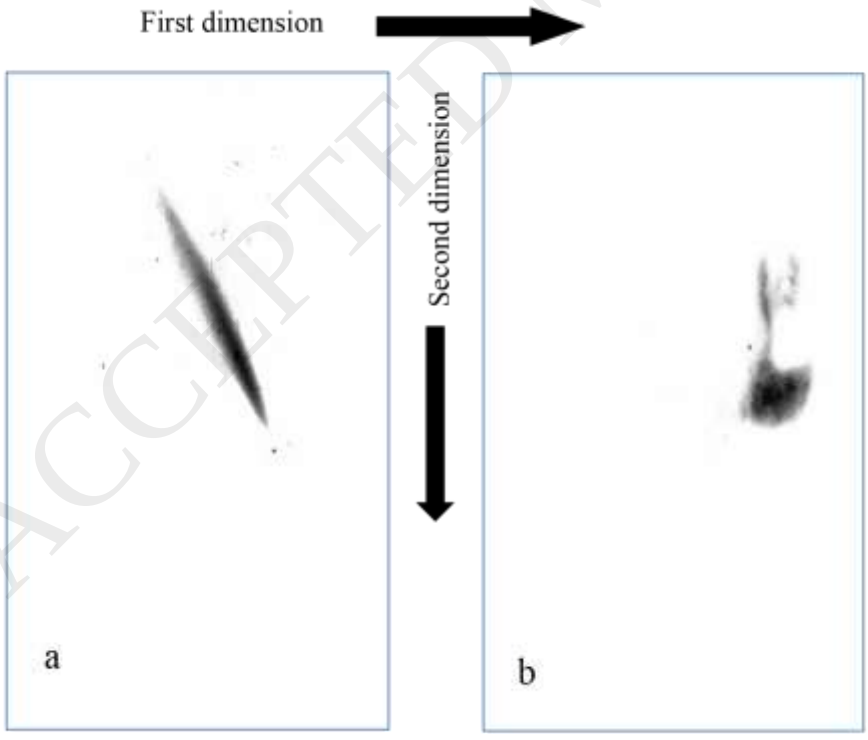

Fig 6. Relative expression levels of circRNAs following RNase R treatment determined by qPCR using divergent (D) primers in MIMV-infected and uninfected maize. Three biological and two technical replicates were used. CircRNA levels were calculated relative to convergent primers of reference gene Cullin-1 isoform X1 (CULF: 5´-GAAGAGCCGCAAAGTTATGG-3´ and CULR: 5´- ATGGTAGAAGTGGACGCACC-3´) in samples without RNase R treatment. Name of samples refers to the name of primers (Table 1). The abbreviations indicate circRNAs 2D: 2:3952580-3952697, 4D: 4:166090900-166091022, 42D: 4:180319497-180319700, 6D: 6:163859492-163859800 and 62D: 6:109834012-109834503.

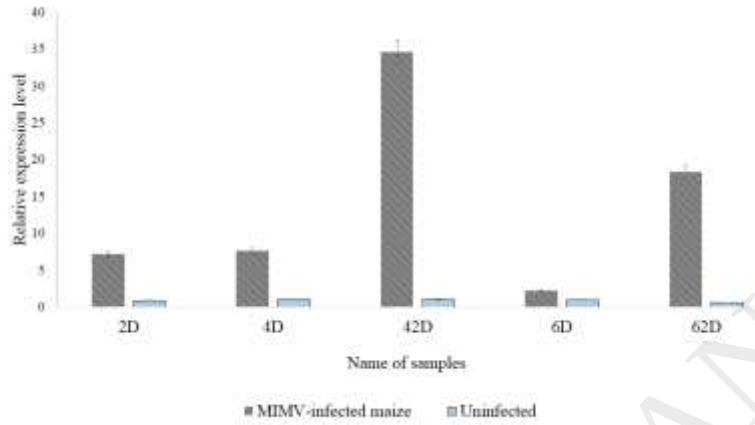

Tables

Table 1. List of convergent and divergent circular RNA primers

Primer set number	**CircPrimer***	**Primer sequence 5' to 3'**
1	2CF	GAAGTAGGGGAAGAGGAGGG
	2CR	GGCGTCGTGGAGCTACAG
2	2DF	GCTGCAGGTTGAGGCTGTA
	2DR	GGCTGTGTTTCCGGACGG
3	4CF	TCCACATGTATCGCCATTTCG
	4CR	GCAGGAGAAGATCAGGAGCA
4	4DF	GCTCCTGATCTTCTCCTGCA
	4DR	GCCAGCCACTCCTAAAGG
5	42CF	TCTCCAGTTCTCCACCTTGC
	42CR	CTGCGGAGGATGAGGTAGAC
6	42DF	GGCGTTCCCGTCGCTGTCGCCGGA
	42DR	GAGACTGGAGAGGGAGATGC
7	6CF	GTCAGACACGAGGAGCTCTT
	6CR	AGTAGTACCATTACCGCCGT
8	6DF	GAGAGGGCCAAGAGAGCAG
	6DR	TGACGTCTCCTGTTTCACCA
9	62CF	TGGCCAAGAGAACTGCATTG
	62CR	TCTGTGTTTGGTGGGGTCTT
10	62DF	GCAGGAATCTTGGCGTTGAA
	62DR	GGCCAAAACCTGAAAACAAGC
*** C = convergent primer and D = divergent primer.**		

Table 2. Predicted microRNA targets for circRNAs in maize

Name of circRNA	Lowest E-value	Name of target microRNA	Max miRNA-circRNA nt sequence complementarity (%)
3:172341356-172341457*	5.08E-03	MIR408b	94.44
2:1923979-1970968	6.74E-03	MIR399a	100
6:168207956-168208082	6.56E-03	MIR397b	100
1:59133633-59133788	1.95E-04	MIR396f	100
1:59133633-59133776	1.78E-04	MIR396f	100
7:140181432-140181631	3.07E-03	MIR396e	94.74
1:299505065-299505279	5.27E-07	MIR396d	90.91
3:203517163-203517271	4.51E-04	MIR394a	95
3:59632396-59632591	3.01E-03	MIR319a	95.24
3:217618989-217680689	2.98E-07	MIR2275c	87.5
7:130347160-130391269	4.68E-03	MIR2275c	88.24
4:180319497-180319700	3.14E-03	MIR2118f	100
2:219185798-219185962	8.81E-03	MIR2118d	90
2:55894943-55895081	2.08E-03	MIR172e	100
6:146402289-146402395	1.54E-03	MIR171g	100
5:76848856-76848977	1.80E-03	MIR167h	100
1:272191046-272191163	6.03E-03	MIR166n	90
2:243860850-243861152	1.38E-03	MIR166a	88
2:204819373-204819539	8.93E-03	MIR166a	82.14
1:16961034-16961336	4.80E-03	MIR164e	84.62
2:189269044-189269177	6.97E-03	MIR164c	100
5:161330154-161330300	5.22E-05	MIR160e	95.45
2:55895017-55895119	9.93E-06	MIR159e	100
2:55894943-55895132	5.61E-06	MIR159e	100
2:55894982-55895132	4.41E-06	MIR159e	100
4:220718016-220718134	6.09E-03	MIR159e	100
5:162606203-162606544	1.56E-03	MIR159e	90.91
5:222622088-222622199	1.63E-03	MIR159d	91.3
10:4273184-4273390	2.62E-04	MIR159c	95.24
10:4273184-4273390	2.62E-04	MIR159c	95.24
9:132779074-132779240	8.93E-03	MIR159a	100
4:83387567-83387709	7.51E-03	MIR156k	100
4:83387586-83387707	6.27E-03	MIR156k	100

*Number of maize chromosome: start nt location- end nt location